JACS
JOURNAL OF THE AMERICAN CHEMICAL SOCIETY

Article

Affinity-guided oxime chemistry for selective protein acylation in live tissue systems

Tomonori Tamura, Zhining Song, Kazuma Amaike, Shin Lee, Sifei Yin, Shigeki Kiyonaka, and Itaru Hamachi

J. Am. Chem. Soc., **Just Accepted Manuscript** • DOI: 10.1021/jacs.7b07339 • Publication Date (Web): 15 Sep 2017

Affinity-guided oxime chemistry for selective protein acylation in live tissue systems

Tomonori Tamura,[1] Zhining Song,[1] Kazuma Amaike,[1] Shin Lee[1], Sifei Yin[2], Shigeki Kiyonaka[1] and Itaru Hamachi[1,3]

[1]Department of Synthetic Chemistry and Biological Chemistry, Graduate School of Engineering, Kyoto University, Katsura, Nishikyo-ku, Kyoto 615-8510, JAPAN

[2]Magdalene College, University of Cambridge

[3]CREST(Core Research for Evolutional Science and Technology, JST), Sanbancho, Chiyodaku, Tokyo, 102-0075, JAPAN

Correspondence should be addressed to I.H. (ihamachi@sbchem.kyoto-u.ac.jp).

Abstract

Catalyst-mediated protein modification is a powerful approach for the imaging and engineering of natural proteins. We have previously developed affinity-guided 4-dimethylaminopyridine (DMAP) (AGD) chemistry as an efficient protein modification method using a catalytic acyl transfer reaction. However, because of the high electrophilicity of the thioester acyl donor molecule, AGD chemistry suffers from nonspecific reactions to proteins other than the target protein in crude biological environments, such as cell lysates, live cells, and tissue samples. To overcome this shortcoming, we here report a new acyl donor/organocatalyst system that allows more specific and efficient protein modification. In this method, a highly nucleophilic pyridinium oxime (PyOx) catalyst is conjugated to a ligand specific to the target protein. The ligand-tethered PyOx selectively binds to the target protein and facilitates the acyl transfer reaction of a mild electrophilic *N*-acyl-*N*-alkylsulfonamide acyl donor on the protein surface. We demonstrated that the new catalytic system, called AGOX (affinity-guided oxime) chemistry, can modify target proteins, both in test tubes and cell lysates, more selectively and efficiently than AGD chemistry. Low-background fluorescence labeling of the endogenous cell-membrane proteins, carbonic anhydrase XII and the folate receptor, in live cells allowed for the precise quantification of diffusion coefficients in the protein's native environment. Furthermore, the excellent biocompatibility and bioorthogonality of AGOX chemistry were demonstrated by the selective labeling of an endogenous neurotransmitter receptor in mouse brain slices, which are highly complicated tissue samples.

Introduction

The methodology to selectively label proteins of interest (POIs) with synthetic probes in live cells or tissue samples is becoming increasingly important for the investigation of the structure, function, dynamics, and localization of individual proteins in their native environment.[1] A wide variety of chemical strategies for the selective labeling of proteins have been developed in the last two decades.[1,2] Catalyst-mediated protein labeling is one of the most powerful and successful of these strategies in chemical biology. For example, the copper (I)-catalyzed azide-alkyne cycloaddition reaction, known as "click chemistry", is now the most widely used bioorthogonal reaction for protein bioconjugation.[3] Other transition metal catalysts, including palladium, rhodium, ruthenium, and iridium, have also proven to be useful for modifying proteins with excellent chemoselectivity both *in vitro* and in bacterial cells.[4] However, despite several successful examples,[5] transition metal catalyst-mediated protein labeling in cellular contexts often suffers from cytotoxicity derived from high concentrations of the metal catalyst, which have hampered biological applications in the more sensitive and complicated mammalian cells. In addition, most of these methods, in principle, require the incorporation of bioorthogonal reactive handles into POIs as coupling substrates via genetic engineering, because it is impossible to selectively modify unengineered natural proteins. This requirement might potentially interfere with the physiological conditions in living systems. Some recent studies have reported that protein ligand-tethered transition metal catalysts can selectively modify native proteins in crude biological samples.[6] However, few reports have demonstrated the use of transition metal-mediated affinity labeling in live-cell contexts.[7]

As an alternative to transition metals, organocatalysts are also promising for use in protein labeling.[8] We have previously reported an organocatalyst-based protein labeling method,

termed affinity-guided 4-dimethylaminopyridine (DMAP) (AGD) chemistry (**Figure 1a**).[9] In this strategy, the affinity ligand–DMAP conjugate selectively binds to the target protein, and the DMAP moiety facilitates an acyl transfer reaction from thiophenyl ester acyl donors containing a reporter tag to the nucleophilic group of an amino acid (e.g. the ε-amino group of Lys and phenol group of Tyr) in the vicinity of the ligand-binding pocket of the POIs. Using this proximity-driven protein modification, we achieved the selective fluorescence labeling of membrane receptors endogenously expressed on living cell surfaces.[9c,9e] However, several issues regarding the biocompatibility and bioorthogonality of AGD chemistry still remain to be challenging (**Figure 1a**): (1) Basic pH conditions (pH > 8) are necessary for efficient labeling because of the low nucleophilicity of DMAP at neutral pH. (2) Undesired (non-catalytic) acylation to non-target proteins inevitably occurs in crude biological environments because of the inherently high electrophilicity of thioester acyl donors. Thus, the reaction is usually carried out at low temperature (~4 °C) to minimize non-specific labeling. (3) Thioester acyl donors are readily decomposed by esterases in biological samples, which requires high concentrations of reagents. These shortcomings have hampered the application of AGD chemistry to more complicated and delicate biological samples, such as live tissues. Therefore, the development of a new acyl donor/organocatalyst pair applicable for affinity-guided protein labeling is desirable.

Here, we describe the use of pyridinium oxime as a nucleophilic acyl transfer catalyst for proximity-driven protein labeling with a mild electrophilic *N*-acyl-*N*-alkylsulfonamide acyl donor under physiological conditions (**Figure 1b**). This new catalytic system, called AGOX (affinity-guided oxime) chemistry, allowed more efficient labeling of natural proteins in test tubes and cell lysates than AGD chemistry. AGOX chemistry was also applicable to the selective labeling and fluorescent imaging of endogenous cell-membrane proteins in live cells, providing a

tool for the precise evaluation of diffusion coefficients in their native environments. Furthermore, the improved biocompatibility and bioorthogonality enabled the selective modification of an endogenous neurotransmitter receptor in acutely prepared mouse brain slices.

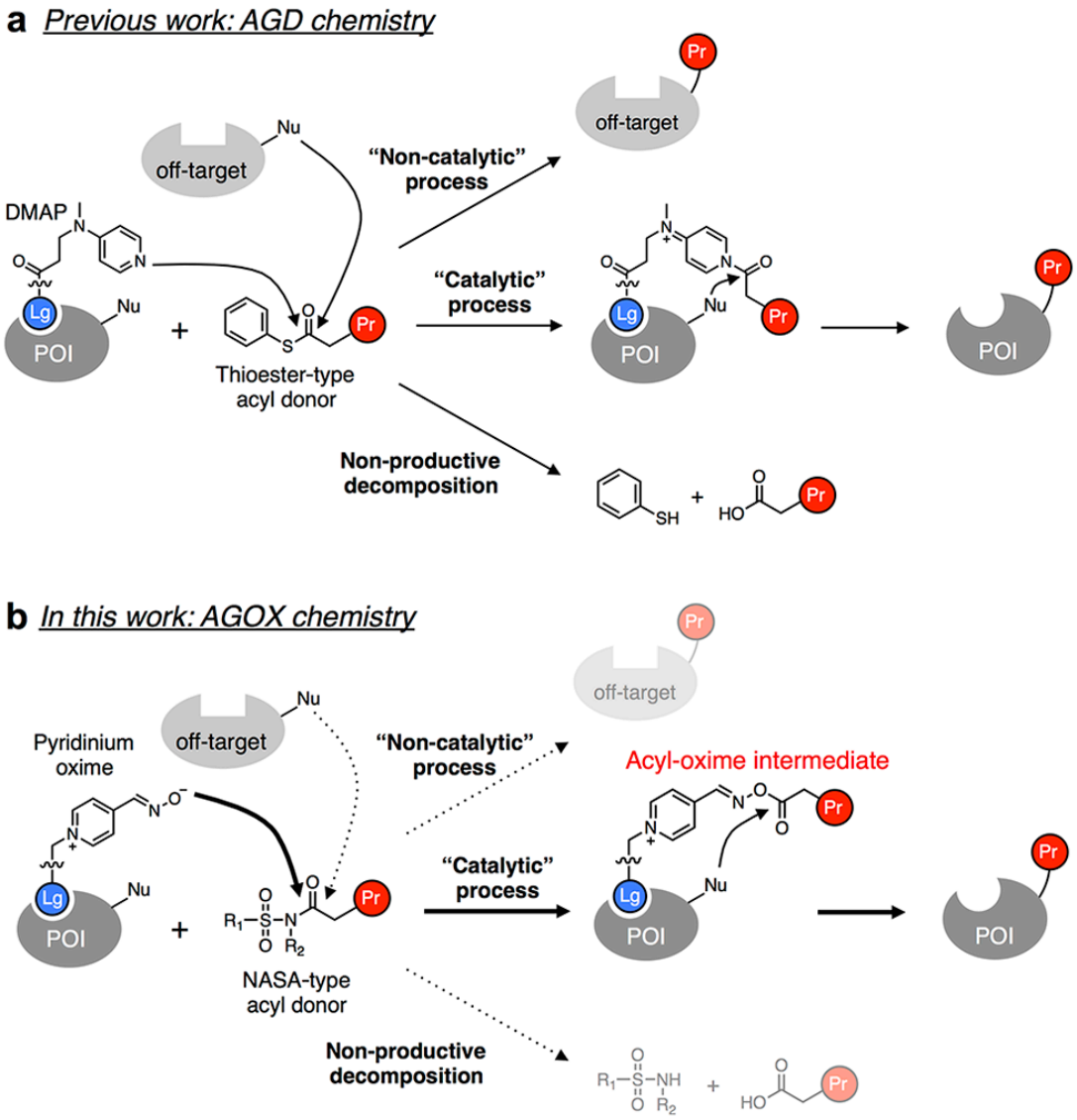

Figure 1 Schematic illustration of protein chemical labeling by (a) affinity-guided DMAP (AGD) chemistry and (b) affinity-guided oxime (AGOX) chemistry. DMAP, 4-dimethylaminopyridine; NASA, *N*-acyl-*N*-alkyl sulfonamide; POI, protein of interest; Pr, probe; Lg, ligand; Nu, nucleophilic amino acid.

Results and discussion

1. Design and *in vitro* evaluation of nucleophilic oxime catalysts

We initially investigated the potential of pyridinium aldoxime (PyOx) derivatives as new candidates for acyl-transfer catalysts for our affinity-guided strategies. PyOx compounds are important antidotes for reactive organophosphate poisoning owing to their strong catalytic ability to hydrolyze the *O*-phosphorylated serine of acetylcholinesterase (AChE).[10] PyOx compounds have reported pKa values close to neutral pH (7–8.5), and the corresponding oximate ions exhibit a high nucleophilicity compared with conventional oxygen-based nucleophiles with similar basicity.[11] In addition, *O*-acylated oximes are known to be good acyl-transfer reagents.[12] Given these properties, we envisioned that a ligand-tethered PyOx derivative would be able to activate a weakly electrophilic acyl donor at neutral pH and transfer the acyl group to a nucleophilic residue on a target protein. This method may also reduce undesired background signals arising from non-catalytic labeling.

To test this hypothesis, we compared the nucleophilicity of PyOx with DMAP and a benzaldoxime (pKa ~10)[13] at neutral pH (pH 7.2, 37 °C). The hydrolysis of *p*-nitrophenylacetate (PNPA), a model electrophile, catalyzed by 4-pyridinium aldoxime derivative **1**, DMAP, or benzaldoxime **2** was spectroscopically monitored (**Figure 2a, Figure S1**).[14] As shown in **Figure 2b**, compound **1** promoted hydrolysis more efficiently than DMAP. On the other hand, **2** showed no catalytic effect, indicating that the lower pKa value of PyOx **1** is essential for the high nucleophilicity. The second order rate constant (k_2) was determined to be 2.14 ± 0.08 $M^{-1}s^{-1}$ for **1** and 0.237 ± 0.001 $M^{-1}s^{-1}$ for DMAP (**Figure 2c**), indicating that the nucleophilicity of 4-pyridinium aldoxime **1** is 9-fold higher than that of DMAP under neutral aqueous conditions.

We next examined the protein-labeling capability of the PyOx group conjugated to a

protein ligand. FKBP12 was employed as the target protein,[9c] and thus a ligand-tethered PyOx reagent **3** containing SLF (synthetic ligand of FKBP12) was designed and synthesized (**Figure 2d**). The linker length of **3** between the PyOx moiety and SLF was referred to a previously developed AGD catalyst for FKBP12 (SLF-tri DMAP **8**, **Figure S6**).[9c, 15]

In vitro labeling was performed by incubation of purified FKBP12 (5 μM, Mw: 11,914) with SLF-PyOx **3** and a fluorescein (FL)-tethered thioester acyl donor (FL-SPh **4**)[9] (**Figure 2d**) in buffer solution (pH 7.2) at 37 °C. As shown in **Figure 2e**, the molecular mass corresponding to FL-labeled FKBP12 (Mw: 12,357) was observed by MALDI-TOF mass spectrometry. No significant labeling occurred without **3** or in the presence of excess amount of rapamycin, a competitive ligand, in the 4 h incubation, indicating that the labeling reaction was driven by specific protein–ligand recognition. Thus, ligand-tethered PyOx can activate a thioester acyl donor and efficiently transfer the acyl group to nucleophilic amino acids of FKBP12 through a proximity effect.

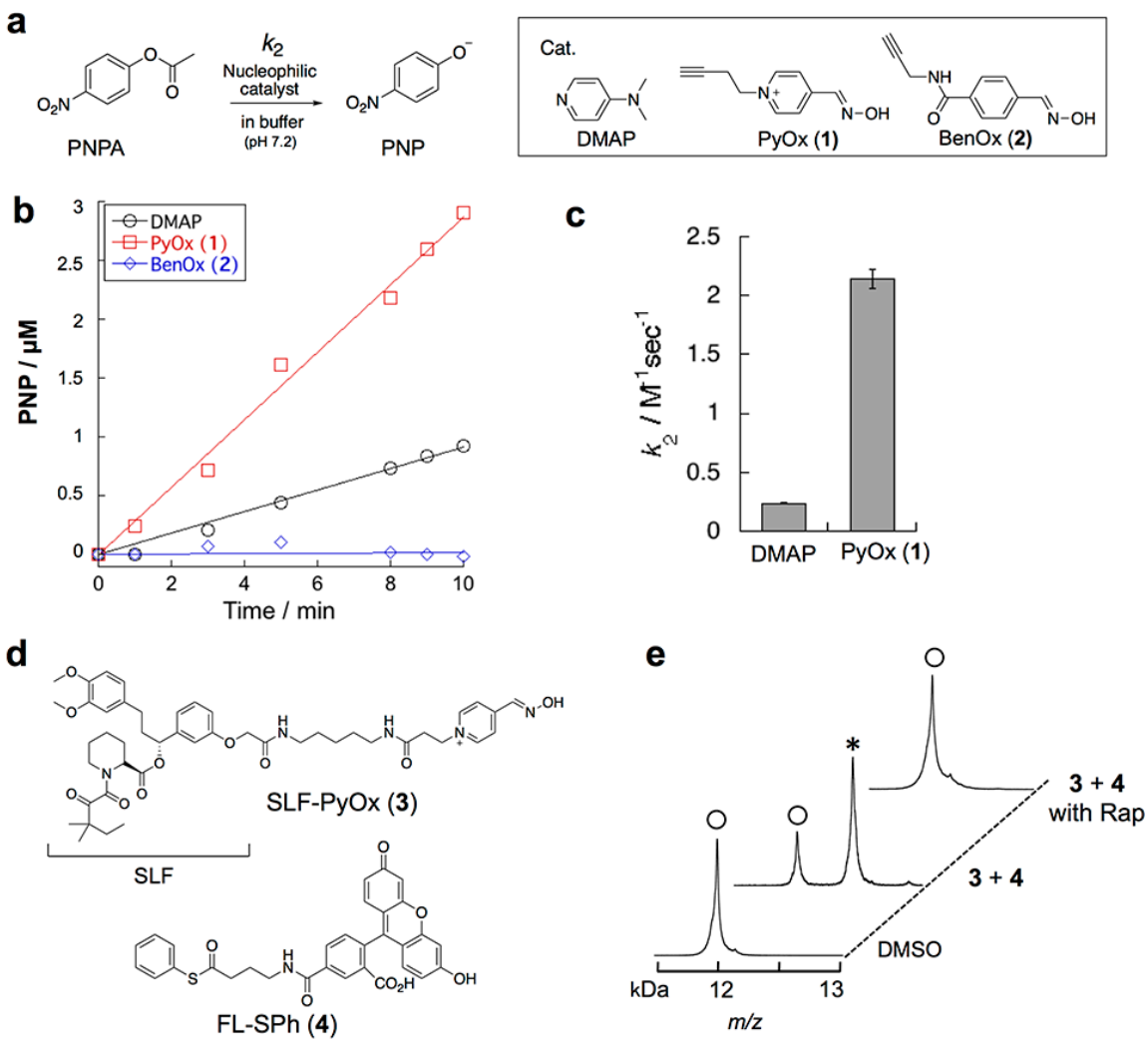

Figure 2 *In vitro* evaluation of the nucleophilicity of PyOx under neutral pH conditions. (a) Catalytic hydrolysis of PNPA. PNPA, *p*-nitrophenylacetate; PNP, *p*-nitrophenol. (b) Time courses of the hydrolysis of PNPA in the presence of DMAP (○), PyOx **1** (□), or benzaldoxime (BenOx) **2** (◇). Reaction conditions: 200 μM PNPA, 20 μM catalyst, 50 mM HEPES buffer, pH 7.2, 37 °C. The reaction was monitored by the absorbance at 348 nm with a UV-Vis spectrometer. (c) k_2 values for the hydrolysis of PNPA with DMAP and PyOx **1**. (d) Molecular structure of SLF-PyOx **3** and FL-SPh **4**. (e) MALDI-TOF mass analysis of FKBP12 labeling with SLF-PyOx **3** and FL-SPh **4**. Reaction conditions: 5 μM FKBP12, 5 μM SLF-PyOx **3**, 50 μM FL-SPh **4**, 50 μM rapamycin (Rap), 50 mM HEPES buffer, pH 7.2, 37 °C. ○, native FKBP12 (M.W. 11,914); *, FL-labeled FKBP12 (M.W. 12,357).

2. NASA derivatives as new acyl donors

We next explored more suitable acyl donors, than the previously used thioesters, which may reduce the background reactions of undesired protein labeling in crude biological environments. We focused on *N*-acyl-*N*-alkyl sulfonamide (NASA) as a unique acyl-donor scaffold, which is used in solid-phase peptide synthesis as Kenner's safety-catch linker (**Figure 3**)[16]. NASA was expected to have the following advantages over conventional acyl donors: (1) as there is no NASA scaffold in biological systems, it should be less susceptible to enzymatic degradation, and (2) the electrophilicity of the acyl group of NASA is able to be finely tuned by the substitution of electron-withdrawing group (EWG) at aryl sulfonyl (R1) and/or *N*-alkyl (R2) moieties. To optimize the reactivity of NASA acyl donors, we prepared five compounds **5a**–**5e** containing a biotin tag (Bt) and varied the EWGs at R1 and R2, including nitrile, nitro, and fluoride groups (**Figure 3**). Non-catalytic (background) reactions of these acyl donors with FKBP12 were initially evaluated. FKBP12 (5 μM) was mixed with Bt-NASA **5a**–**5e** (50 μM) or Bt-thioester acyl donor (Bt-SPh **6**) (50 μM), followed by MALDI-TOF mass analysis. While no labeling occurred even after 24 h for compounds **5a**–**5d**, labeled peaks corresponding to non-catalytic reactions were detected for **5e** (~9%), and for Bt-SPh **6** (~100%) (**Figure 4a**). We thus excluded the Bt-NASA **5e** because of this higher reactivity.

We then performed FKBP12 labeling with Bt-NASA **5a**–**5d** catalyzed by SLF-PyOx **3**. As shown in **Figure 4b, 4c** and **Figure S2**, efficient labeling took place only with Bt-NASA **5a**, which contains a *p*-nitrophenyl group in both the aryl sulfonyl (R1) and *N*-alkyl (R2) positions. This reaction was completely abolished in the presence of a competitive inhibitor (FK506), demonstrating that the labeling was greatly facilitated by an affinity-driven proximity effect (**Figure S2**). We also found that the labeling yield exceeded 100% (i.e. multiple labeling

occurred) after 1 h (**Figure 4b** and **4c**), which indicated that the PyOx-mediated FKBP12 labeling catalytically proceeded with the NASA acyl donor. Use of **5b**–**5d** showed lower yields and slower reaction kinetics (**Figure 4b, 4c** and **Figure S3**), probably because the electrophilicity of these compounds was too weak. Given these results, *N*-(4-nitrobenzyl)-*N*-(4-nitrophenyl) sulfonamide was selected as the optimal acyl donor for PyOx-mediated protein labeling.

The stability of the optimal NASA was evaluated by a hydrolysis assay (**Figure 4d**, **Figure S4**, and **Table S1**). The half-life for autolysis in aqueous buffer (pH 7.2) was determined to be 81 h for the FL-NASA **7** (**Figure 3**), which is longer than that of the FL-SPh **4** ($t_{1/2}$ = 60 h). More importantly, FL-NASA **7** was also stable even in the presence of an esterase ($t_{1/2}$ = 55 h), in contrast with the rapid hydrolysis of FL-SPh **4** ($t_{1/2}$ = 0.5 h). Thus, we envisioned that the NASA acyl donor should be suitable for protein labeling under crude biological conditions.[17]

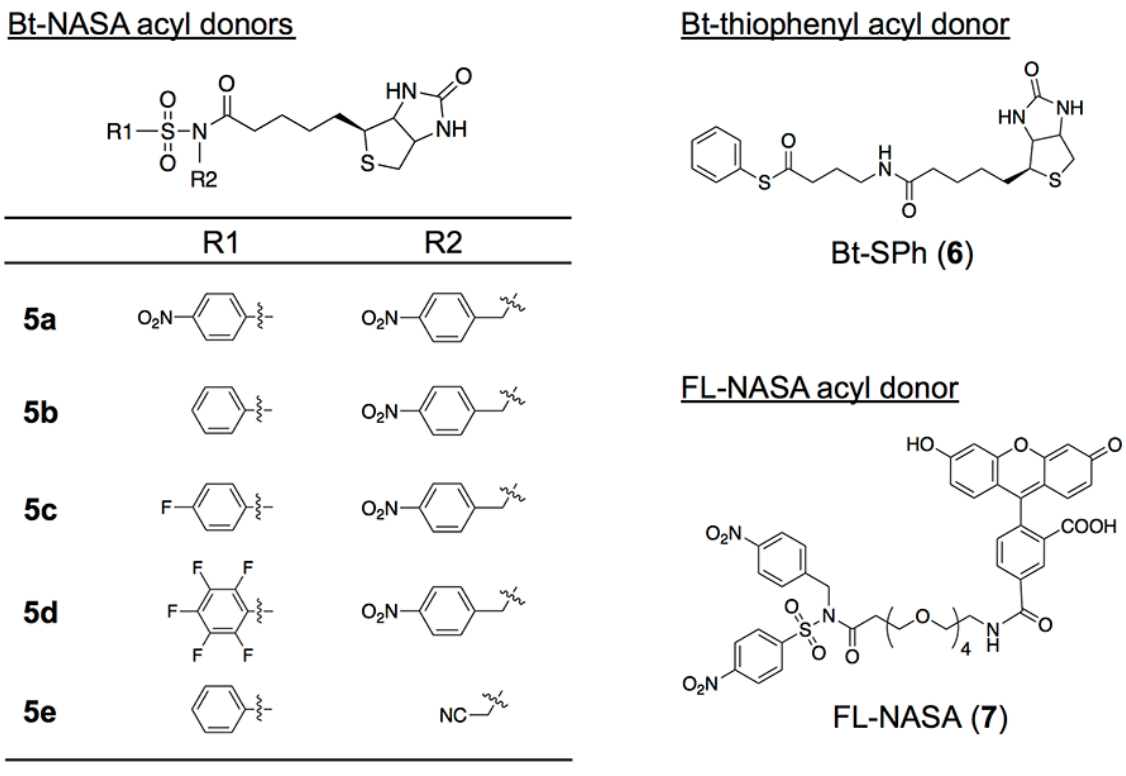

Figure 3 Molecular structures of NASA and thioester acyl donors. Bt, biotin; FL, fluorescein.

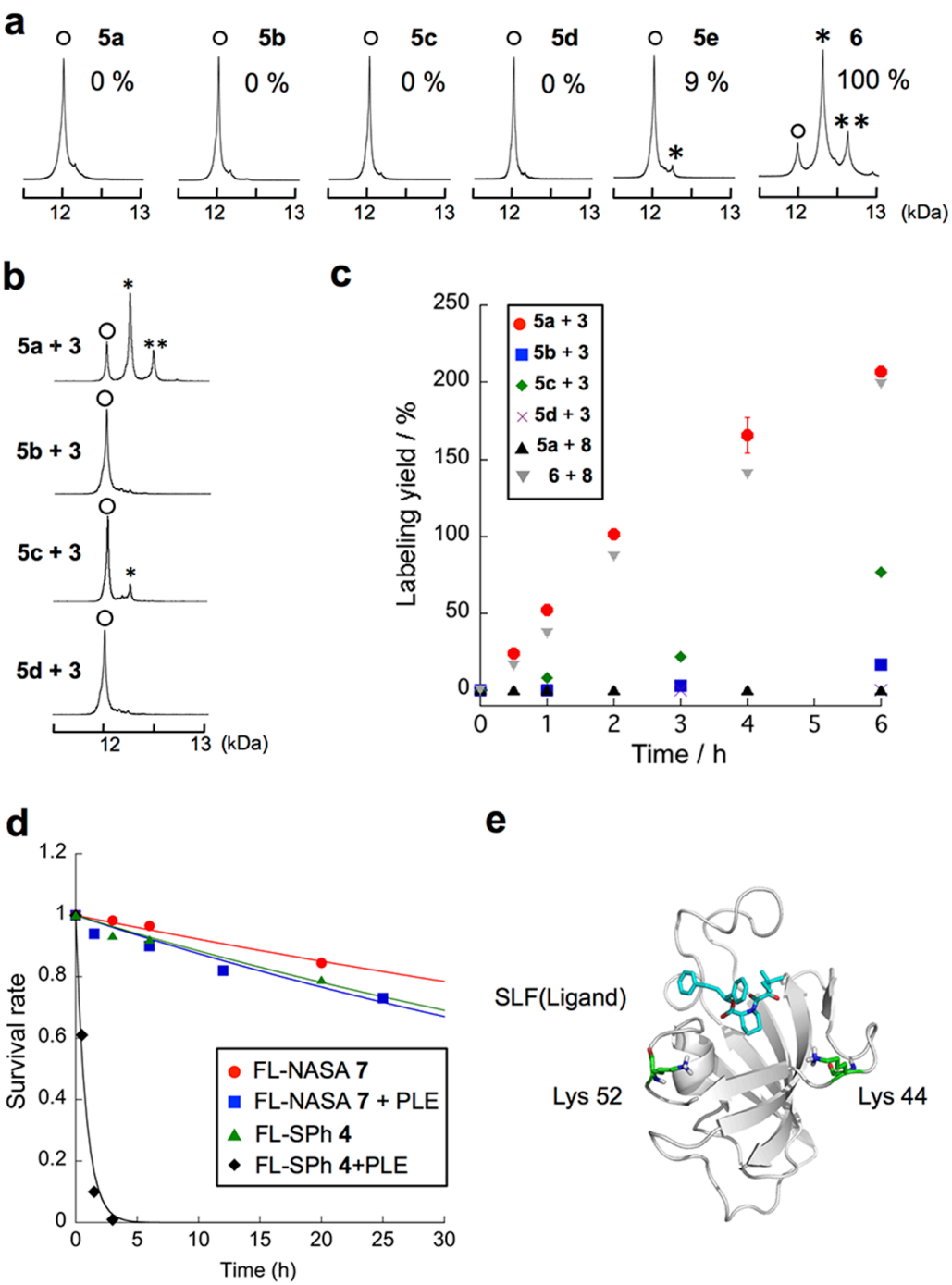

Figure 4 Reaction properties of NASA acyl donors. (a, b) MALDI-TOF mass analysis of FKBP12 labeling with Bt-NASA **5a**–**5e** or Bt-SPh **6** in the absence (a) and presence (b) of SLF-PyOx **3**. Reaction conditions: 5 μM FKBP12, 50 μM acyl donor, 5 μM SLF-PyOx **3**, 50 mM HEPES buffer, pH 7.2, 37 °C. ○, native FKBP12 (M.W. 11,914); *, single Bt-labeled FKBP12 (M.W. 12,140); **, double Bt-labeled FKBP12 (M.W. 12,366). (c) Time courses of reaction yields of FKBP12 labeling by Bt-NASA **5a**–**5d** with SLF-PyOx **3**, and Bt-NASA **5a** or Bt-SPh **6** with SLF-triDMAP **8**. (d) Time course plots of the hydrolysis of FL-NASA **7** and FL-SPh **4** in the absence (**7**, ●; **4**, ▲) or presence (**7**, ■; **4**, ◆) of porcine liver esterase (PLE). Survival rates at several time points were calculated by the integration of the signal in HPLC analyses (**Figure S4**), and fitted using a single-phase exponential decay model to obtain the half-life for each acyl donor in aqueous buffer. (e) The crystal structure of the FKBP12-SLF complex (PDB ID:1FKG)

3. *In vitro* protein labeling using AGOX chemistry

The labeling method using the PyOx catalyst **3**/NASA acyl donor **5a** pair showed sufficient (2 h, ~100 %) FKBP12 labeling under neutral pH (7.2), and the labeling yield and kinetics was comparable to (or slightly better than) AGD chemistry with SLF-triDMAP **8** (**Figure S6**) and Bt-SPh **6** under the same condition (**Figure 4c**). On the other hand, the reaction using SLF-triDMAP **8** and NASA **5a** resulted in no labeled products under the same conditions (**Figure 4c**). This contrast can be ascribed to the fact that the PyOx catalyst, but not the triDMAP group, can efficiently activate the NASA acyl donor, highlighting the high nucleophilicity of PyOx even at neutral pH. The pH dependence of AGOX chemistry is shown in **Figure S7**. The labeling occurred around physiological pH (6.5−8.0), with an increased rate at higher pH, suggesting that deprotonation of both aldoxime and certain nucleophilic amino acid side chains may contribute to the accelerated acyl transfer reaction at the basic pH. The labeled products were stable at 37 °C in the pH range (pH 6.5−8.0) at least for 30 h (**Figure S8**).

The sites of FKBP12 labeled by the SLF-PyOx **3**/FL-NASA **7** pair were identified by conventional peptide mapping analysis. FL-labeled FKBP12 was digested with trypsin, and the resultant peptide fragments were analyzed by HPLC and MALDI-TOF MS/MS. As shown in **Figure 4e**, and **Figure S9–S11**, Lys44 (79%) and Lys52 (21%), which are both the nearest lysine residues from the SLF ligand in the binding pocket (11.8 Å and 11.9 Å, respectively), were modified with FL. This identification was strongly supported by the labeling of two FKBP12 mutants (K44R and K52A), in which the labeling yields were substantially diminished (**Figure S12**).

According to the affinity-guided catalyst strategy, the target protein for labeling can be readily altered by switching the ligand part of the ligand-tethered PyOx. In carbonic anhydrase II

(CAII) labeling, phenylsulfonamide (SA) was selected as the affinity ligand[18] (**Figure 5a**) and the effective *in vitro* labeling of CAII was performed by the pair of SA-PyOx **9** and FL-NASA **7** (**Figure S13**). We found that increasing the number of PyOx moieties (divalent-PyOx) in the ligand-tethered catalyst, SA-diPyOx **10**, enhanced the reaction rate like the example of AGD chemistry (**Figure S13**).[9c] We also determined the amino acids of CAII modified with **10** and **7** (**Figure S14**). Notably, in addition to lysine (Lys169, 76%), a serine residue (Ser2, 24%) was identified as an amino acid targetable by AGOX chemistry. The resultant Ser2 ester bond is chemically stable at 37 °C in a buffer (pH 8.0) at least for 30 h (**Figure S15**).

To compare the target selectivity of AGOX with AGD chemistry, we conducted CAII labeling in cell lysates. A HeLa cell lysate containing CAII (0.5 μM) was incubated for 3 h with PyOx catalysts (**9** or **10**) and FL-NASA **7**, or SA-triDMAP **11** and FL-SPh **4**. As shown in **Figure 5b**, the diPyOx **10**/NASA **7** pair selectively labeled CAII without noticeable background (lane 5). In contrast, multiple bands attributed to non-specific (non-catalytic) labeling were detected for the triDMAP **11**/thioester **4** pair (lane 8). The target-selective labeling of AGOX chemistry was also observed for FKBP12 labeling in cell lysate (**Figure S16**). Taken together, it is clear that the newly-developed PyOx catalyst/NASA acyl donor pair exhibited higher labeling efficiency and selectivity compared with AGD chemistry in cell lysates.

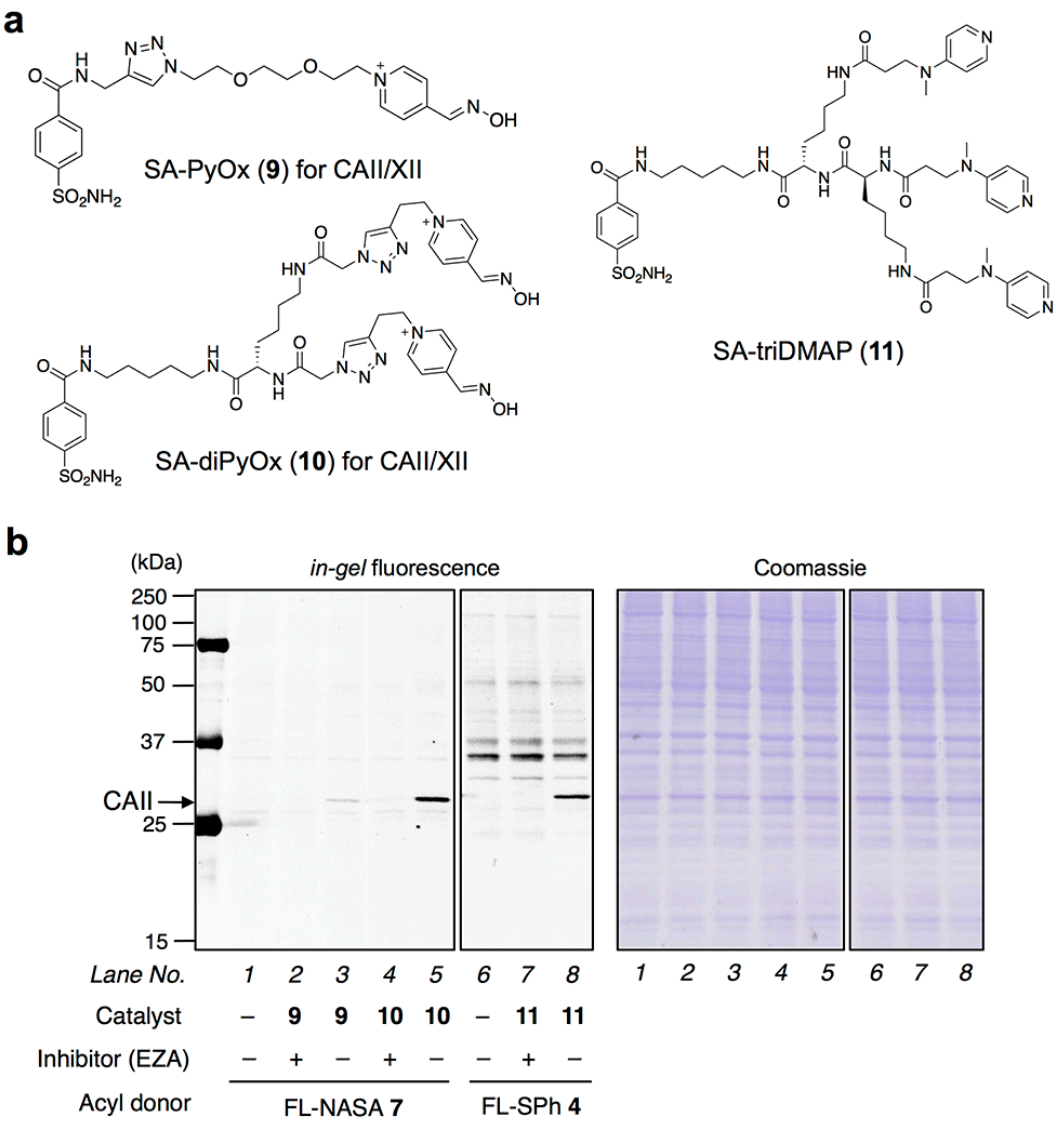

Figure 5 CAII labeling in cell lysates. (a) Molecular structures of SA-PyOx **9**, SA-diPyOx **10**, and SA-triDMAP **11** for CAII and CAXII labeling. (b) SDS-PAGE analysis by in gel fluorescence imaging and Coomassie brilliant blue staining. HeLa cell lysate (protein concentration: 1.0 mg/mL) was mixed with recombinant CAII (final concentration, 0.5 μM), and incubated with acyl donors (5 μM) and catalysts (0.5 μM) in 50 mM HEPES buffer, pH 7.2, 37 °C. EZA, Ethoxzolamide.

4. Selective labeling of endogenous membrane proteins in live cells

Having established the AGOX chemistry, we next applied this strategy to the chemical modification of endogenous membrane proteins expressed on live cells. Membrane-bound carbonic anhydrase XII (CAXII) was chosen as a target protein.[19] Mono- (**9**) and diPyOx (**10**) containing the SA ligand, and the less cell-permeable FL-NASA **7** were employed for CAXII

labeling. A549 cells were incubated in culture medium containing catalyst (5 μM) and **7** (5 μM) at 37 °C.[20] The cells were subsequently washed with phosphate buffered saline (PBS), lysed and analyzed by western blotting using anti-CAXII and anti-FL antibodies.[21] As shown in lane 3 of **Figure 6a**, a strong band corresponding to FL-labeled CAXII was observed with SA-diPyOx **10** and FL-NASA **7** after 1h incubation. This band was not detected when the labeling was performed in the absence of **10** or in the presence of excess EZA (ethoxzolamide), a strong inhibitor of CAXII. Time-course experiments showed that the reaction with SA-diPyOx **10** and FL-NASA **7** reached a plateau at approximately 3 h, and the labeling yield was estimated to be 48% of the entire population of CAXII (**Figure S17** and **S18**). Compared with diPyOx **10**, the labeling efficiency of mono-PyOx **9** was 2.5-fold lower (**Figure S19**). We also compared the target selectivity and labeling efficiency of AGOX with AGD chemistry in live cells. As shown in lanes 5–7 of **Figure 6a**, FL-SPh **4** promiscuously reacted with many proteins even in the absence of the AGD catalyst, leading to more background signals. In contrast, such non-catalytic reactions did not occur using FL-NASA **7**, because of the well-controlled electrophilicity. Moreover, the labeling yield of CAXII with PyOx/NASA was 1.2-fold greater than with AGD chemistry (lanes 3 and 6 in **Figure 6a**). These results clearly verified that AGOX chemistry is superior to our previously reported AGD chemistry,[9] in terms of both selectivity and efficiency of membrane protein labeling in live cells.

Fluorescent live imaging of endogenous CAXII with the Oregon Green (OG)-NASA acyl donor **12** strongly supported the above-mentioned western blotting results (**Figure 6b**).[22] Strong fluorescence of OG-labeled CAXII was observed from the plasma membrane area of live A549 cells by confocal laser-scanning microscopy (CLSM) (**Figure 6c**). This fluorescence was not detected in the absence of catalyst or in the presence of a competitive inhibitor (EZA), which

indicated that the fluorescence from the cell surface is predominantly attributed to OG-labeled CAXII. Similar to CAXII, the endogenous folate receptor (FR) on live KB cells was selectively labeled and visualized using **13** containing the methotrexate (MTX) ligand and OG-NASA **12** (**Figure 6d** and **Figure S21**).[23]

Taking advantage of the selective incorporation of a fluorophore into endogenous membrane proteins with a high signal-to-noise ratio, we sought to apply the AGOX labeling method to quantitatively analyze the protein dynamics in their native environments. After protein labeling using AGOX chemistry in live cells, fluorescence recovery after photobleaching (FRAP) was conducted to evaluate the protein diffusion kinetics on the cell surface.[24] The fluorescence recovery was monitored at 37 °C after bleaching the fluorescence of OG-labeled CAXII or FR on a selected area (diameter: 3.0 μm) of the cell membrane with a confocal laser beam (**Figure 6e**). As shown in **Figure 6f**, typical recovery curves, because of the lateral diffusion of the corresponding proteins, were obtained for OG-labeled CAXII on A549 cells and FR on KB cells. The lateral diffusion coefficients (*D*) were determined, by fitting the raw data according to the previously reported Soumpasis mathematical equation,[31] to be $(7.5 \pm 1.4) \times 10^{-2}$ $\mu m^2/s$ for CAXII and 0.11 ± 0.02 $\mu m^2/s$ for FR (**Figure 6f**). The obtained *D* value for FR was consistent with the reported value for GFP-fused FR (ca. 0.06 $\mu m^2/s$)[25], validating our FRAP experiment. There are no reports for the diffusion kinetics of CAXII. To the best of our knowledge, this is the first report measuring the diffusion dynamics of endogenous FR and CAXII in live cells. Overall, the combination of the PyOx-mediated labeling method with FRAP analysis provides a powerful platform to investigate the diffusion dynamics of endogenous membrane proteins in their native habitats with minimal perturbation.

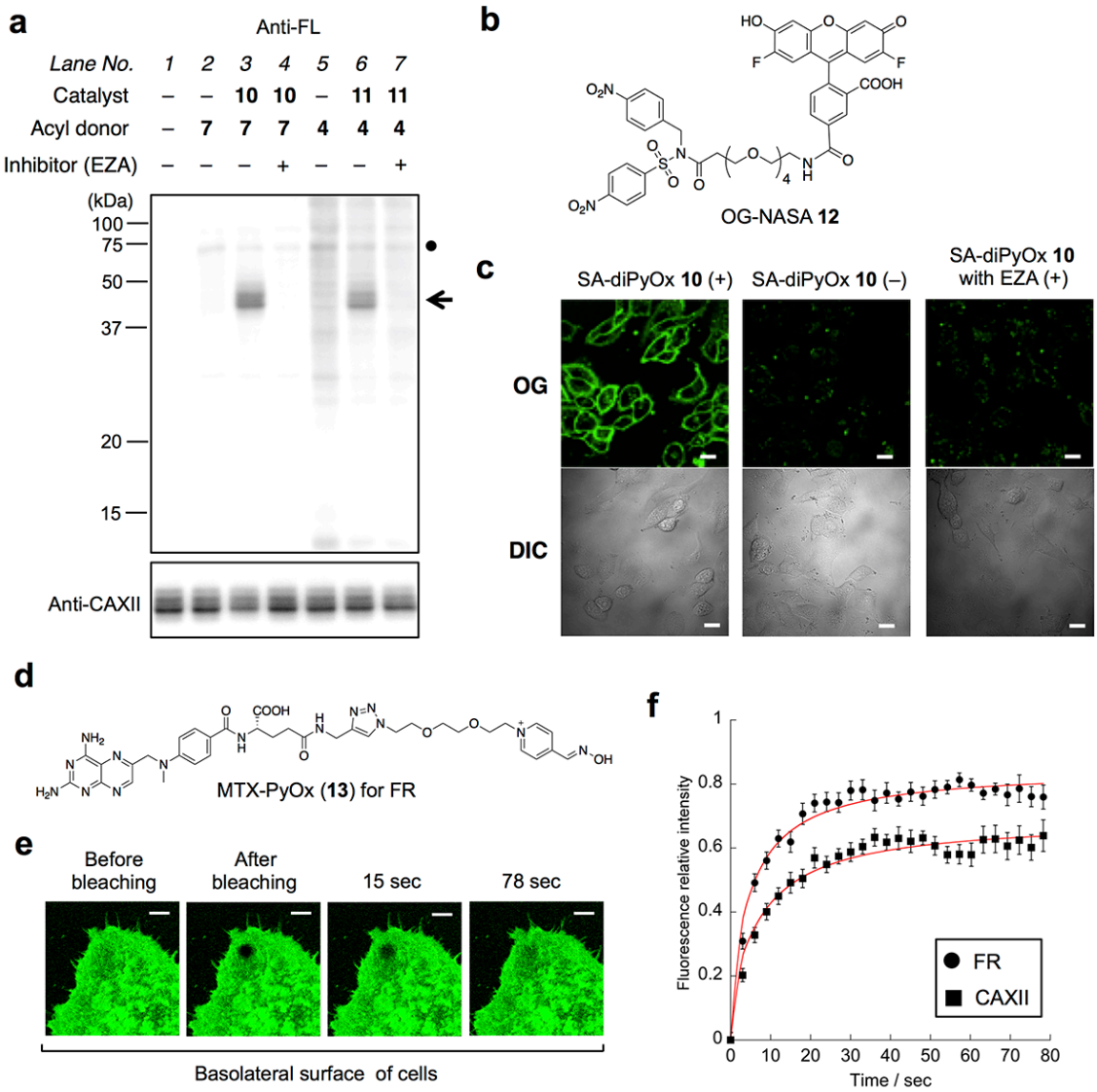

Figure 6 Specific labeling and dynamic analyses of endogenous membrane proteins using AGOX chemistry in living cells. (a) Western blotting analysis of CAXII labeling. A549 cells were treated with catalysts (5 μM) and acyl donors (5 μM) for 1 h at 37 °C in DMEM-HEPES buffer (pH 7.4). After washing, the cells were lysed and analyzed by western blotting using anti-FL and anti-CAXII antibodies. The band with a black arrow corresponds to CAXII and the black dot (●) corresponds to non-specifically-labeled bovine serum albumin (BSA) derived from the culture medium. (b) Molecular structure of OG-appended NASA acyl donor **12**. (c) Confocal micrograph images of A549 cells labeled with SA-diPyOx **10** and OG-NASA **12**. A549 cells were treated with **10** (5 μM) and **12** (5 μM) for 1 h at 37 °C in DMEM-HEPES buffer (pH 7.4) (left). As negative controls, the labeling reaction was performed without **10** (middle) or in the presence of EZA (50 μM) (right). Scale bars, 20 μm. (d) Molecular structure of MTX-PyOx **13** for FR labeling. (e) Representative images of a confocal FRAP experiment. Endogenous FR on KB cells was labeled with MTX-PyOx **13** and OG-NASA **12** for 1 h at 37 °C in culture medium. After washing the cells 3 times with DMEM-HEPES, FRAP experiments were conducted. Diameter of bleach circle, 3.0 μm. Scale bars, 5 μm. (f) Kinetics of recovery for OG-labeled FR (●) in KB cells and OG-labeled CAXII (■) in A549 cells at 37 °C. Each plot shows the mean ± SD from 12–15 cells. The calculated D values were $(7.5 \pm 1.4) \times 10^{-2}$ $\mu m^2/s$ for CAXII and 0.11 ± 0.02 $\mu m^2/s$ for FR.

5. Endogenous AMPAR labeling in brain tissues

Finally, we applied the AGOX chemistry to label native neurotransmitter receptor proteins located in brain hippocampal and cerebellar tissue slices, which are more complicated and delicate biological samples than cultured cells (**Figure 7a**). Glutamate receptors are endogenously expressed in the excitatory neurons of the brain and classified into several groups depending on their ligand recognition properties and relevant functions. Among them, the α-amino-3-hydroxy-5-methyl-4-isoxazolepropionic acid (AMPA)-type glutamate receptors (AMPARs), which are composed of heteromeric tetramers of four subunits (GluA1–GluA4), are essential for synaptic plasticity and play crucial roles in memory formation. We selected the AMPARs as target proteins in the brain slices and designed the corresponding PyOx catalyst **14** containing di-PyOx and 6-pyrrolyl-7-trifluoromethyl-quinoxaline-2,3-dione (PFQX) as a ligand (K_i =170 nM) (**Figure 7b**).[26]

Covalent FL-modification of AMPAR by the **14/7** pair was initially confirmed by a labeling experiment using living HEK293T cells transiently expressing the GluA2 subtype, a major subtype of the AMPARs in the brain (**Figure 7c**). Western blotting analysis showed that selective labeling of AMPAR occurred and this was inhibited by the addition of NBQX (a competitive antagonist of the AMPARs). The labeling sites on the AMPAR were identified using a recombinant of the ligand-binding domain of GluA2 to be Lys470 and Lys677, both located at the entrance of the ligand-binding pocket (**Figure S22** and **S23**).

These results encouraged us to investigate chemical modification of endogenous AMPARs in brain slices. Acutely prepared hippocampal slices from mice brains were incubated in buffer containing PFQX-diPyOx **14** (1 μM) and FL-NASA **7** (1 μM) at 20 °C for 30 min. The tissues were then washed with buffer and lysed, followed by western blotting analysis. As shown

in **Figure 7d**, while a few bands attributable to off-target labeling were detected, a strong band corresponding to FL-labeled AMPARs was predominant in the presence of PFQX-diPyOx **14** and FL-NASA **7**.[27] This band was completely abolished by co-incubation with NBQX, strongly indicating selective labeling of AMPARs in hippocampal slices. It should be noted that AGD chemistry failed to label AMPARs in brain slices because of heavy nonspecific background labeling (**Figure 7d**). In the cerebellum, neurons expressing AMPARs are highly covered with glial cells, and the expression level of AMPARs is less than in hippocampal neurons.[28] Even in these conditions, successful AMPARs selective labeling using the PyOx **14**/NASA **7** pair was able to be achieved in cerebellar slices (**Figure S24**). These results highlight the sufficient bioorthogonality and broad utility of AGOX chemistry in complex tissue samples.

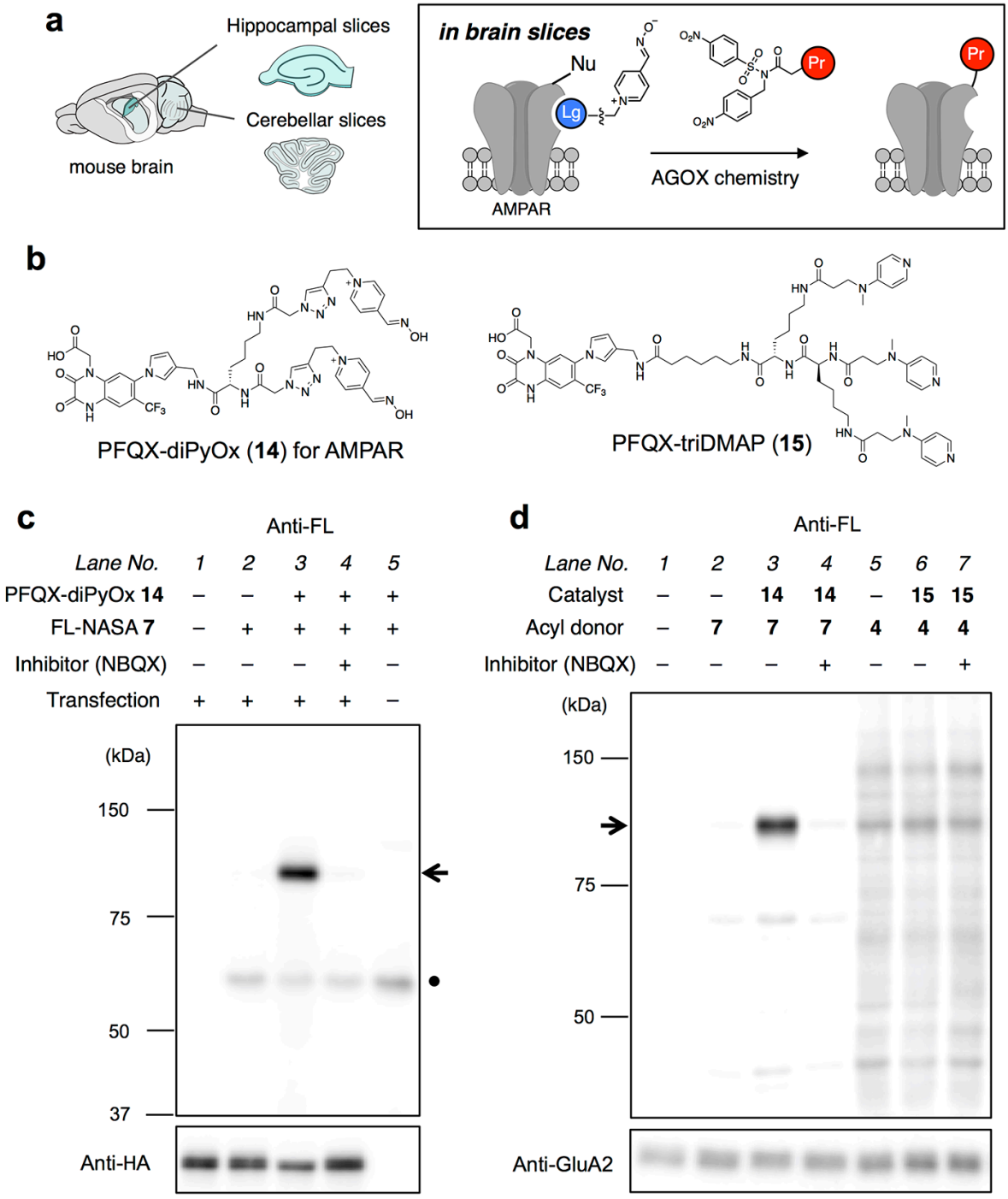

Figure 7 Selective labeling of endogenous neurotransmitter receptors in brain slices. (a) Schematic illustration of chemical protein labeling in brain slices by AGOX chemistry. (b) Molecular structures of PFQX-diPyOx (**14**) and PFQX-triDMAP (**15**) for AMPAR labeling. (c) Western blotting analysis of AMPAR labeling in HEK293T cells transiently expressing AMPAR (HA-tagged GluA2). HEK293T cells transiently expressing AMPAR were treated with catalysts (5 μM) and acyl donors (5 μM) in the absence or presence of 50 μM NBQX in serum free DMEM. The cell lysates were analyzed by western blot using anti-FL or anti-HA antibodies. The band with a black arrow corresponds to AMPAR and the black dot (●) corresponds to non-specifically-labeled BSA derived from the culture medium. (d) Western blot analyses of AMPAR labeling in hippocampal slices. Hippocampal slices were treated with catalysts (1 μM) and acyl donors (1 μM) in the absence or presence of 100 μM NBQX in ACSF buffer. The cell lysates were analyzed by western blotting using anti-FL or anti-GluA2 antibodies.

Conclusions

In conclusion, we have developed a new affinity-guided chemistry for protein labeling through precisely controlling both the nucleophilicity of the catalyst and the electrophilicity of the acyl donor. AGOX chemistry showed remarkably improved selectivity and bioorthogonality as compared with AGD chemistry, which enabled the quantitative evaluation of endogenous protein dynamics in their native environments and the selective labeling of a naturally occurring neurotransmitter receptor in brain tissue slices.

It should be pointed out that, on the other hand, the AGOX chemistry has still limitations. In particular, this method is not applicable to intracellular proteins so far. This is partially due to the low membrane permeability of the pyridinium cation moiety of the catalyst (**Figure S25**). We are now working on developing an oxime catalyst with both a high membrane permeability and a strong nucleophilicity. Besides, ligand-directed protein labeling approaches generally need a specific ligand for POIs, which may limit the scope of targetable proteins. However, compared with ligand-directed chemistry, such as ligand-directed tosyl (LDT)[29] or acyl imidazole (LDAI) chemistry[26,30], the most significant advantage of the affinity-guided catalyst strategy is that protein or peptide ligands, as well as small-molecules, can be employed as target-recognition modules. This is because the affinity-guided catalyst can minimize the protein (ligand)-attacked decomposition of labeling reagents. Therefore, a variety of protein and peptide ligands (e.g. cytokines, toxins, complements, lectins, and small antibodies) may be used in PyOx-conjugates, which not only expands the range of available target proteins, but also enables diverse applications of this method. Given the previous examples of AGD chemistry[9d,9e], for instance, the AGOX-mediated protein labeling should be more applicable to detect protein-protein interactions such as antigen-antibody and lectin-glycoprotein interactions, as a

powerful alternative to photo-crosslinking strategy. Such research are now underway in our group.

Materials and Methods

Synthesis.

The synthesis of reagents **4**, **6** and **8** has been reported previously.[9b, 9c] All other synthetic procedures and compound characterizations are described in the Supporting Information.

General materials and methods for the biochemical/biological experiments.

Unless otherwise noted, all proteins/enzymes and reagents were obtained from commercial suppliers (Sigma-Aldrich, Tokyo Chemical Industry (TCI), Wako Pure Chemical Industries, Sasaki Chemical, Bio-Rad, or Watanabe Chemical Industries) and used without further purification. UV-vis absorption spectra were acquired on a Shimadzu UV-2550 spectrophotometer. Matrix-assisted laser desorption/ionization time-of-flight mass spectrometry (MALDI-TOF MS) spectra were recorded on an Autoflex III instrument (Bruker Daltonics) using α-cyano-4-hydroxycinnamic acid (CHCA) or sinapic acid as the matrix. SDS-polyacrylamide gel electrophoresis (SDS-PAGE) and western blotting were carried out using a Bio-Rad Mini-Protean III electrophoresis apparatus. Fluorescence gel images and chemical luminescent signals using Chemi-Lumi one (Nacalai Tesque) or ECL Prime (GE Healthcare) were acquired with an imagequant LAS4000 (Fujifilm). Cell imaging was performed with a confocal laser-scanning microscope (CLSM, Olympus, FV1000) using 60× objectives, and images were analyzed using accompanying ASW 3.0 Viewer software. Reversed-phase HPLC (RP-HPLC) was carried out on a Hitachi LaChrom L-7100 system equipped with a LaChrom L-7400 UV detector, and a YMC-Pack ODS-A column (5 μm, 250 × 4.6 mm) at a flow rate of 1.0 mL/min. UV detection was at 220 nm. All runs used linear gradients of acetonitrile containing 0.1% TFA (solvent A) and 0.1% aqueous TFA (solvent B).

Determination of the rate constants of nucleophilic reaction with PNPA.

To a solution of PNPA (*p*-nitrophenylacetate) (30 μM) in PBS buffer (pH 7.4) was added a significant excess of DMAP or PyOx **1** (6, 9, 12, 15 mM) at 37 °C. Reaction progress was monitored by the absorbance at 348 nm or 400 nm with UV-vis spectrometer. The concentrations of PNP (*p*-nitrophenol) at various time points were determined by the absorbance at 400 nm using the molar absorption coefficient of PNP ($\varepsilon_{400\ nm}$ = 8084 $cm^{-1}M^{-1}$).[14] The pseudo-first-order rate constants (k_{obsd}) at different concentrations of DMAP or **1** were obtained by fitting the data to a single-phase exponential growth model. These rate constants at various concentrations of DMAP or **1** were fitted by linear regression to determine the second order rate constants (k_2).

Preparation of recombinant FKBP12 (wild type, K44R and K52A)

Recombinant human FKBP12 (wild type) was obtained as described previously.[29b] The K44R and K52A mutants of FKBP12 were generated by QuickChange II XL site-directed mutagenesis kit (Agilent) using primers 5'-CTCCCGGGACAGAAACAGGCCCTTTAAGTTTATG-3' and 5'-CATAAACTTAAAGGGCCTGTTTCTGTCCCGGGAG-3' for the K44R, and

5'-GTTTATGCTAGGCGCGCAGGAGGTGATCCGAG-3' and 5'-CTCGGATCACCTCCTGCGCGCCTAGCATAAAC-3' for the K52A, with a pGEX-ST plasmid encoding wild-type FKBP12 (a kind gift from Dr. Shirakawa) as a template. Plasmids were verified by sequencing and transformed into BL21 DE3 codon plus RIL cells. The cells were grown in LB media containing ampicillin at 37 °C to an optical density (660 nm) of 0.6, at which time the expression of protein was induced by the addition of 1 mM IPTG. After growth for an additional 5−7 h at 30 °C, the cells were harvested by centrifugation. The cell pellets were resuspended in a lysis buffer (50 mM Tris-HCl, 300 mM NaCl, 1 mM DTT, 1 mM EDTA, 1 mM PMSF, pH 8.0), and lysed by sonication. The proteins were purified from the soluble fraction of the lysate using a glutathione-Sepharose column chromatography (GE Healthcare) and dialyzed against 50 mM Tris, 150 mM NaCl, 1 mM DTT, pH 8.0. The GST tag in the fusion protein was cleaved with SENP protease at 4 °C for 30 h. The resulting (tag-free) FKBP12 mutants were purified by gel filtration chromatography on HiLoad 16/600 Superdex 75 prep grade (GE healthcare, Little Chalfont, UK) with a flow rate of 0.8 mL/min using an ÄKTA purifier system equilibrated with 50 mM HEPES, 100 mM NaCl, pH 8.0. The fractions were monitored at 280 nm, collected using Frac-920, and analyzed the purity by SDS-PAGE. The concentrations of FKBP12 were determined by bicinchroninic acid (BCA) protein assay (Thermo).

FKBP12 Labeling *in vitro*.

Purified FKBP12 (5 μM) was incubated with acyl donors (50 μM) in the presence of catalyst (5 μM) in HEPES buffer (50 mM, pH 7.2) at 37 °C. Control labeling reactions in the presence of excess rapamycin or FK506 (10 equiv), or without catalyst were also carried out. Aliquots at different time points were taken, and the labeling yields were determined by MALDI-TOF MS (matrix: CHCA)

CAII labeling *in vitro*.

Human carbonic anhydrase II (CAII) was purchased from SIGMA-Aldrich, and used without further purifcation. The concentrations of CAII were determined by absorbance at 280 nm using a molar extinction coefficient of 54 000 M^{-1} cm^{-1} in 50 mM HEPES buffer (pH 7.4). CAII (10 μM) was incubated with acyl donor **7** (100 μM) in the presence of catalyst **9** or **10** (10 μM) in HEPES buffer (50 mM, pH 7.2) at 37 °C. Control labeling reactions in the presence of excess EZA (10 equiv) or without catalyst were also carried out. Aliquots at different time points were taken, and the labeling yields were determined by MALDI-TOF MS. (matrix: Sinapic acid).

CAII labeling in HeLa cell lysate.

HeLa cells (1×10^7 cells) were suspended in HEPES buffer (50 mM, pH 7.2) containing 1% protease inhibitor cocktail set III (Calbiochem) and lysed by Potter-Elvehjem homogenizer at 4 °C. The lysate was centrifuged at 16000 × g for 3 min, and the supernatant was collected. Protein concentration was determined by BCA assay and adjusted to 1.0 mg/mL. This solution was incubated with CAII (0.5 μM), acyl donor (5 μM) and catalyst (0.5 μM) for 3 h at 37 °C. The reaction mixture was mixed with the same volume of 2×sample buffer (pH 6.8, 125 mM Tris–HCl,

20% glycerol, 4% SDS, 0.01% bromophenol blue, 250 mM DTT) and incubated for 1 h at 25 °C. The samples were subjected to SDS-PAGE, and the gel was analyzed by fluorescence gel imager (LAS4000) and Coomassie Brilliant Blue (CBB) stain.

Evaluation of stabilities of acyl donors.

Acyl donor **7** or **4** (20 μM) and internal standard (Terephthalic acid, 500 μM) were incubated with or without Pig liver esterase (PLE, 0.1 μM) in HEPES buffer (50 mM, pH 7.2) at 37 °C. Samples at different time points were taken and analyzed by RP-HPLC.

Peptide Mapping of the FL-Labeled FKBP12.

Recombinant FKBP12 (20 μM) was incubated with acyl donor **7** (50 μM) in the presence of catalyst **3** (20 μM) in HEPES buffer (50 mM, pH 7.2) at 37 °C. After 4h, the labeled FKBP12 was purified by size-exclusion chromatography using a TOYOPEARL HW-40F column and dialyzed against HEPES buffer (50 mM, pH 8.0) with a Spectra/Por dialysis membrane (MWCO: 3,000). To this solution, urea (at a final concentration of 2 M) and Trypsin (Trypsin /substrate ratio = 1/10 (w/w)) were added. After incubation at 37 °C for 20 h, the digested peptides were separated by analytical RP-HPLC. The collected fractions were analyzed by MALDI-TOF MS (matrix: CHCA) and the labeled fragment was further characterized by MALDI-TOF-TOF MS/MS analysis.

Chemical labeling of CAXII in A549 cells.

A549 cells (1.5×10^5 cells) were cultured in Dulbecco's modified Eagle's medium (DMEM) supplemented with 10% fetal bovine serum (FBS, Gibco), penicillin (100 units/ml), streptomycin (100 mg/ml), and amphotericin B (250 ng/ml), and incubated under the hypoxic condition (<0.1% O_2) generated with AnaeroPack (Mitsubishi Gas Chemical Company) for 1 day. The cells were then incubated in FBS-free DMEM containing catalyst (5 μM) and acyl donor (5 μM) at 37 °C. As control experiments, the labeling was conducted in the presence of EZA (50 μM) or without catalyst. For western blot analysis, after chemical labeling, the cells were washed three times with PBS, and then RIPA buffer (pH 7.4, 25 mM Tris–HCl, 150 mM NaCl, 0.1% SDS, 1% Nonidet P-40, 0.25% deoxycholic acid) was added containing 1% protease inhibitor cocktail set III (Calbiochem). The lysed sample was collected and centrifuged (15,200 *g*, 10 min at 4 °C). The supernatant was mixed with the same volume of 2×sample buffer and incubated for 1h at 25 °C. The samples were subjected to SDS-PAGE and electro-transferred onto an Immun-Blot PVDF membrane (Bio-Rad). The labeled CAXII was detected by chemiluminescence analysis using rabbit anti-fluorescein antibody (Abcam, ab19491) and anti-rabbit IgG-HRP conjugate (Santa Cruz, sc-2004). The anti-fluorescein antibody (Abcam, ab19491) was also used for the detection of oregon-green labeled proteins. The immunodetection of CAXII was performed with a rabbit anti-CAXII antibody (Cell Signaling, D75C6) and anti-rabbit IgG-HRP conjugate.

Chemical labeling of FR in KB cells.

KB cells were cultured in folate-free RPMI1640 (Gibco) supplemented with 10% FBS, penicillin (100 units/ml), streptomycin (100 mg/ml), and amphotericin B (250 ng/ml), and incubated in a 5% CO_2 humidified chamber at 37 °C. For the endogenous FR labeling, KB cells (1.5×10^5 cells) were washed three times with folate- and FBS-free RPMI1640. The cells were incubated in folate- and FBS-free RPMI1640 containing catalyst (5 μM) and acyl donor (5 μM) at 37 °C. As control experiments, the labeling was conducted in the presence of folate (50 μM) or without catalyst. After labeling, the cells were washed three times with PBS, and then RIPA buffer was added containing 1% protease inhibitor cocktail set III. The lysed sample was collected and centrifuged (15,200 *g*, 10 min at 4 °C). The supernatant was mixed with the same volume of 2×sample buffer and incubated for 1 h at 25 °C. The samples were analyzed by western blotting using anti-fluorescein/oregon-green antibody, anti-FR antibody (Abcam, ab125030) and anti-rabbit IgG-HRP conjugate.

CLSM imaging

After chemical labeling as described above, the cells were washed 3 times with HBS (20 mM HEPES, 107 mM NaCl, 6 mM KCl, 2 mM $CaCl_2$, and 1.2 mM $MgSO_4$ at pH 7.4). Cells imaging was performed with a confocal microscopy (FV1000, Olympus). The fluorescence images were obtained by excitation at 473 nm and simultaneous detection with 500 – 600 nm emission filter.

FRAP experiment

After labeling of CAXII or FR with oregon green dye as described above, the cells were washed 3 times with HBS. The fluorescence images were obtained by excitation at 473 nm and simultaneous detection with 500 – 600 nm emission filter at 37 °C. Bleaching was performed with a circular spot (diameter 3.0 μm) using the 488nm lines from a 40 mW argon laser operating at 100% laser power for 3 msec. Fluorescence recovery was monitored at low laser intensity at 3 sec intervals. The lateral diffusion coefficient (*D*) was determined by fitting the raw data according to the previously described Soumpasis mathematical equation shown below: [31]

$$frap_{\mathrm{d}}(t) = e^{-\left(\frac{w^2}{2Dt}\right)} \left(\mathrm{I}_0 \left(\frac{w^2}{2Dt}\right) + \mathrm{I}_1 \left(\frac{w^2}{2Dt}\right) \right)$$

where *w* is the radius of the beam.

Chemical labelling of AMPARs in HEK293T cells.

HEK293T cells were incubated in DMEM under 5% CO_2 at 37 °C. Cells were transfected with a pCAGGS plasmid encoding flop form of RNA-edited GluA2 ($GluA2^{flop}$ (R))[26] using the lipofectamine 2000 (Invitrogen) according to the manufacture's instruction and subjected to labeling experiments after 18 h of the transfection. For chemical labeling, the cells expressing GluA2 were washed three times with FBS-free DMEM and treated with catalyst (5 μM) and acyl donor (5 μM) at 37 °C in FBS-free DMEM and incubated for 1 h. As control experiments, the

labeling was conducted in the presence of NBQX (50 μM) or without catalysts. The cells were washed three times with PBS, and then lysed with RIPA buffer as described above. The samples were analyzed by western blotting using anti-fluorescein antibody, anti-HA tag antibody (for AMPAR detection, abcam, ab9110) and anti-rabbit IgG-HRP conjugate.

Chemical labeling and western blot analysis of Hippocampal or cerebellar slices.

Hippocampus or cerebellum (200 μm thickness) was prepared from P14–21 ICR mice. The slices were treated with catalyst (1 μM) and acyl donor (1 μM) in ACSF solution (125 mM NaCl, 2.5 mM KCl, 2 mM $CaCl_2$, 1 mM $MgCl_2$, 1.25 mM NaH_2PO_4, 26 mM $NaHCO_3$, 10 mM D-glucose and 100 mM Picrotoxin) at 20 °C for 0.5 h under 95% O_2/5% CO_2. As control experiments, the labeling was conducted in the presence of NBQX (100 μM) or without catalysts. The slices were then washed with ACSF solution three times and lysed with RIPA buffer containing 1% protease inhibitor cocktail set III. The lysed sample was centrifuged (15,200 *g*, 10 min at 4 °C). The supernatant was mixed with the same volume of 2×sample buffer and incubated for 1 h at 25 °C. The samples were analyzed using anti-fluorescein antibody, anti-GluA2 antibody (abcam, ab20673) and anti-rabbit IgG-HRP conjugate.

Quantitative evaluation of cell-membrane permeability of oxime compounds.

HEK293T cells were incubated in DMEM under 5% CO_2 at 37 °C. Cells were transfected with a pFN21A plasmid encoding HaloTag-FKBP12 (purchased from Promega, clone catalog # FHC02102) using the lipofectamine 2000 according to the manufacture's instruction and subjected to labeling experiments after 38 h of the transfection. The culture media were exchanged with FBS-free DMEM containing oxime-appended substrates (5 μM) and incubated for 1.5 h at 37 °C. After washing with media, the cells were incubated in FBS-free DMEM containing Halo-AcFL (purchased from Promega) (2 μM) for 0.5 h at 37 °C. The cells were washed three times with PBS, and then lysed with RIPA buffer as described above. The samples were analyzed by western blotting using anti-fluorescein antibody, anti-FKBP12 antibody (Abcam, ab2918) and anti-rabbit IgG-HRP conjugate.

Acknowledgements

We thank Naoya Takahashi for preparation of FKBP12 mutants. We also thank Karin Nishimura (Kyoto University) for experimental support of MS measurements. This work was supported by Grant-in-Aid for Young Scientists (B) (15K17884) and The Kyoto University Foundation to T.T., Grant-in-Aid for JSPS Research Fellow to Z.S. (15J07815) and K.A. (17J09635), SUNBOR Grant from Suntory Foundation for Life Sciences and the Takeda Science Foundation to S.K., and the Japan Science and Technology Agency (JST) Core Research for

Evolutional Science and Technology (CREST) to I.H. This work was also supported by a Grant-in-Aid for Scientific Research on Innovative Areas "Chemistry for Multimolecular Crowding Biosystems" (JSPS KAKENHI Grant No. 17H06348).

Competing financial interests

The authors declare no competing financial interests.

References

1. (a) Prescher, J. A.; Bertozzi, C. R. *Nat. Chem. Biol.* **2005**, *1*, 13. (b) Lang, K.; Chin, J. W. *Chem. Rev.* **2014**, *114*, 4764. (c) Ernst, R. J.; Krogager, T. P.; Maywood, E. S.; Zanchi, R.; Beránek, V.; Elliott, T. S.; Barry, N. P.; Hastings, M. H.; Chin, J. W. *Nat. Chem. Biol.* **2016**, *12*, 776. (d)Takaoka, Y.; Ojida, A.; Hamachi, I. *Angew. Chem. Int. Ed. Engl.* **2013**, *52*, 4088.
2. (a) Sletten, E. M.; Bertozzi, C. R. *Angew. Chem. Int. Ed.* **2009**, 48, 6974. (b) Spicer, C. D.; Davis, B. G. *Nat. Commun.* **2014**, *5*, 4740. (c) Chen, X.; Wu, Y.-W. *Org. Biomol. Chem.* **2016**, *14*, 5417.
3. (a)Kolb, H. C.; Finn, M. G.; Sharpless, K. B. *Angew. Chem. Int. Ed.* **2001**, *40*, 2004. (b)Rostovtsev, V.V.; Green, L.G.; Fokin, V.V.; and Sharpless, K.B. *Angew. Chem. Int. Ed.* **2002**, 41, 2596– 2599. (c)McKay, C. S.; Finn, M. G. *Chem. Biol.* **2014**, *21*, 1075.
4. (a) Yang, M.; Li, J.; Chen, P. R. *Chem. Soc. Rev.* **2014**, *43*, 6511. (b) Antos, J. M.; McFarland, J. M.; Iavarone, A. T.; Francis, M. B. *J. Am. Chem. Soc.* **2009**, *131*, 6301. (c) Tilley, S. D.; Francis, M. B. *J. Am. Chem. Soc.,* **2006**, 128, 1080. (d) McFarland, J. M.; Francis, M. B., *J. Am. Chem. Soc.,* **2005**, *127*, 13490. (e) Lin, Y. A.; Chalker, J. M.; Floyd, N.; Bernardes, G. J. L.; Davis, B. G., *J. Am. Chem. Soc.*, **2008**, 130, 9642 (f) Chalker, J. M.; Wood, C. S. C.; Davis, B. G., *J. Am. Chem. Soc.,* **2009**, *131*, 16346. (g) Spicer, C. D.; Triemer, T.; Davis, B. G., *J. Am. Chem. Soc.* **2012**, *134*, 800. (h) Spicer, C. D.; Davis, B. G., *Chem. Commun.,* **2013**, *49*, 2747. (i) Li, J.; Lin, S.; Wang, J.; Jia, S.; Yang, M.; Hao, Z.; Zhang, X.; Chen, P. R. *J. Am. Chem. Soc.* **2013**, *135*, 7330.
5. (a) Hong, V.; Steinmetz, N. F.; Manchester, M.; Finn, M. G. *Bioconjug. Chem.* **2010**, *21*, 1912. (b) Kennedy, D. C.; McKay, C. S.; Legault, M. C. B.; Danielson, D. C.; Blake, J. A.; Pegoraro, A. F.; Stolow, A.; Mester, Z.; Pezacki, J. P., *J. Am. Chem. Soc.,* **2011**, *133*, 17993. (c) Jiang, H.; Zheng, T.; Lopez-Aguilar, A.; Feng, L.; Kopp, F.; Marlow, F. L.; Wu, P., *Bioconjugate Chem.*, **2014**, *25*, 698.
6. (a) Chen, Z.; Popp, B. V.; Bovet, C. L.; Ball, Z. T., *ACS Chem. Biol.*, **2011**, *6*, 920. (b) Chen, Z.; Vohidov, F.; Coughlin, J. M.; Stagg, L. J.; Arold, S. T.; Ladbury, J. E.; Ball, Z. T., *J. Am. Chem. Soc.*, **2012**, *134,* 10138. (c) Ball, Z. T. *Acc. Chem. Res.* **2013**, *46*, 560.(d) Vohidov, F.; Coughlin, J. M.; Ball, Z. T. *Angew Chem Int Ed.* **2015**, *54*, 4587. (e) Ball, Z. T. *Curr. Opin. Chem. Biol.* **2015**, *25*, 98. (f) Sato S.; Nakamura, H. *Angew. Chem. Int. Ed.* **2013**, *52*, 8681.
7. Sato, S.; Morita, K.; Nakamura, H. *Bioconjug. Chem.* **2015**, *26*, 250.
8. Kunishima, M.; Nakanishi, S.; Nishida, J.; Tanaka, H.; Morisaki, D.; Hioki, K.; Nomoto, H., *Chem. Commun.*, **2009**, 37, 5597.
9. (a) Hayashi, T.; Hamachi, I., *Acc. Chem. Res.*, **2012**, 45, 1460. (b) Koshi, Y.; Nakata, E.; Miyagawa, M.; Tsukiji, S.; Ogawa T. and Hamachi, *J. Am. Chem. Soc.*, **2008**, *130*, 245. (c) Wang, H. X.; Koshi, Y.; Minato, D.; Nonaka, H.; Kiyonaka, S.; Mori, Y.; Tsukiji S. and Hamachi, I. *J. Am. Chem. Soc.*, **2011**, *133*, 12220. (d) Hayashi, T.; Sun, Y.; Tamura, T.;

Kuwata, K. Song, Z.; Takaoka, Y. and Hamachi, I. *J. Am. Chem. Soc.,* **2013**, *135*, 12252. (e) Hayashi, T.; Yasueda, Y.; Tamura, T.; Takaoka, Y. and Hamachi, I. *J. Am. Chem. Soc.*, **2015**, *137*, 5372. (f) Song, Z.; Takaoka, Y.; Kioi, Y.; Komatsu, K.; Tamura, T.; Miki, T. and Hamachi, I. *Chem. Lett.*, **2015**, *44*, 333.

10. Jokanović, M.; Prostran, M.. *Curr. Med. Chem.*, **2009**, 16, 2177.
11. Terrier, F.; Maccormack, P.; Kiziliana, E.; Halle, J.; Guirc, D. F.; Lion, C. *J. Chem. Soc. Perkin Trans. 2,* **1991**, 1, 153.
12. Hamuro, Y.; Scialdone, M. A.; DeGrado, W. F. *J. Am. Chem. Soc.* **1999**, *121*, 1636.
13. Han, X.; Balakrishnan, V. K.; Vanloon, G. W.; Buncel, E. *Langmuir* **2006**, *22*, 9009.
14. Bharathi, S.; Wong, P. T.; Desai, A.; Lykhytska, O.; Choe, V.; Kim, H.; Thomas, T. P.; Baker, J. R.; Choi, S. K. *J. Mater. Chem. B,* **2014**, *2*, 1068.
15. For the other catalysts to be mentioned later (**9**, **10**, **13** and **14**), the linker lengths were designed as the PyOx moiety can reach to a few of nucleophilic amino acids (e.g. Lys, Ser, Tyr) locating around the protein surface proximal to the ligand binding site, on the basis of the crystal structures of target proteins.
16. Heidler, P. and Link, A. *Bioorg. Med. Chem.*, **2005,** *13,* 585.
17. We also evaluated the hydrolytic stability of compound **5a**–**5e**. The details are shown in **Figure S5** in the supplementary information.
18. Supuran, C. T. *Nat. Rev. Drug Discov.* **2008**, *7*, 168.
19. Kopecka, J.; Campia, I.; Jacobs, A.; Frei, A. P.; Ghigo, D.; Wollscheid, B.; Riganti, C. *Oncotarget,* **2015**, *6*, 6776.
20. Since a nonspecific reaction to BSA derived from serum in cultured medium competes, the AGOX-mediated labeling was carried out in serum-free medium.
21. To detect the labeling signal from less-abundant proteins, we used more sensitive western blotting analysis with the anti-FL antibody.
22. The labeling selectivity using PyOx **10**/NASA**12** was confirmed by western blotting analysis (**Figure S20**).
23. Matthews, D. A; Alden, R. A; Bolin, J. T.; Freer, S. T.; Hamlin, R.; Xuong, N.; Kraut, J.; Poe, M.; Williams, M.; Hoogsteen, K. *Science* **1977**, *197*, 452.
24. (a) Soumpasis, D. M. *Biophys. J.* **1983**, *41*, 95. (b) Sprague, B. L.; McNally, J. G. *Trends Cell Biol.* **2005**, *15*, 84.
25. Lebreton, S.; Paladino, S. and Chiara Zurzolo, C. *J. Biological Chemistry*, **2008**, *283*, 29545.
26. Wakayama, S.; Kiyonaka, S.; Arai, I.; Kakegawa, W.; Matsuda, S.; Ibata, K.; Nemoto, Y.; Kusumi. A.; Yuzaki, M.; Hamachi, I. *Nat. Commun.*, **2017**, *8*, 14850
27. The endogenous AMPAR is a heteromeric tetramer consisting of a combination of GluA1–GluA4 subunits in brain, and the subunit selectivity was not examined in this study.
28. Lippman-Bell, J. J.; Lordkipanidze, T.; Cobb, N.; Dunaevsky, A. *Neuron Glia Biol.* **2012**, *6,* 193.
29. (a) Tsukiji, S.; Miyagawa, M.; Takaoka, Y.; Tamura, T; Hamachi, I. *Nat. Chem. Biol.* **2009**, *5*, 341. (b) Tamura, T.; Tsukiji, S.; Hamachi, I. *J. Am. Chem. Soc.* **2012**, *134*, 2216. (c)

Tamura, T.; Kioi, Y.; Miki, T.; Tsukiji, S.; Hamachi, I. *J. Am. Chem. Soc.* **2013**, *135*, 6782. (d) Tsukiji, S.; Hamachi, I. *Curr. Opin. Chem. Biol.* **2014**, *21*, 136.

30. (a) Fujishima, S.; Yasui, R.; Miki, T.; Ojida, A.; Hamachi, I. *J. Am. Chem. Soc.* **2012**, *134*, 3961. (b) Miki, T.; Fujishima, S.; Komatsu, K.; Kuwata, K.; Kiyonaka, S.; Hamachi, I. *Chem. Biol.* **2014**, *21*, 1013.

31. Sprague, B. L.; Pego, R. L.; Stavreva, D. A.; McNally, J. G. *Biophys. J.* **2004**, *86,* 3473.

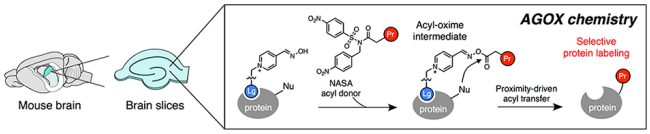
Mouse brain
Brain slices
AGOX chemistry
Acyl-oxime intermediate
Selective protein labeling
NASA acyl donor
Proximity-driven acyl transfer
protein
Nu
Pr

TOC

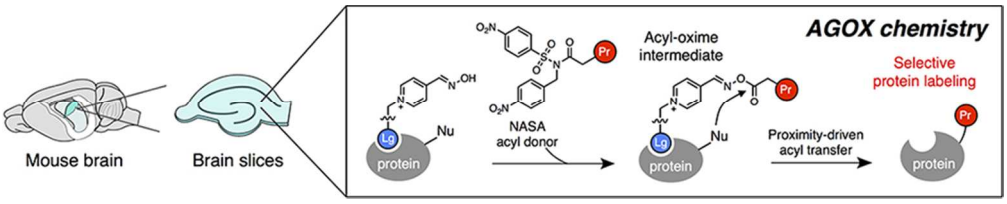

TOC

80x15mm (300 x 300 DPI)